International Journal of Fluid Machinery and Systems
Vol. 9, No. 2, April-June 2016
DOI: http://dx.doi.org/10.5293/IJFMS.2016.9.2.143
ISSN (Online): 1882-9554

Original Paper

A Study on the Multi-Objective Optimization of Impeller for High-Power Centrifugal Compressor

Hyun-Su Kang[1] and Youn-Jea Kim[2]

[1]Graduate School of Mechanical Engineering, Sungkyunkwan University
2066, Seobu-ro, Suwon, 16419, hskang1504@skku.edu
[2] School of Mechanical Engineering, Sungkyunkwan University
2066, Seobu-ro, Suwon, 16419, yjkim@skku.edu

Abstract

In this study, a method for the multi-objective optimization of an impeller for a centrifugal compressor using fluid-structure interaction (FSI) and response surface method (RSM) was proposed. Numerical simulation was conducted using ANSYS CFX and Mechanical with various configurations of impeller geometry. Each design parameter was divided into 3 levels. A total of 15 design points were planned using Box-Behnken design, which is one of the design of experiment (DOE) techniques. Response surfaces based on the results of the DOE were used to find the optimal shape of the impeller. Two objective functions, isentropic efficiency and equivalent stress were selected. Each objective function is an important factor of aerodynamic performance and structural safety. The entire process of optimization was conducted using the ANSYS Design Xplorer (DX). The trade-off between the two objectives was analyzed in the light of Pareto-optimal solutions. Through the optimization, the structural safety and aerodynamic performance of the centrifugal compressor were increased.

Keywords: Centrifugal compressor, Shape optimization, Response surface method, Isentropic efficiency, Fluid-structure interaction

1. Introduction

The centrifugal compressor is the main industrial fluid machine that converts mechanical energy into fluid pressure and kinetic energy through a high-velocity rotating impeller. In general, a centrifugal compressor consists of an inducer, an impeller, a diffuser, and a volute. The shape of the impeller blade is a significant element affecting the aerodynamic performance of centrifugal compressor. Since an impeller receives fluid pressure load and centrifugal force during operation, its structural safety needs to be evaluated. Thus, it becomes necessary to analyze the effects of the impeller blade shape on its aerodynamic performance and structural safety by using fluid-structure interaction (FSI).

For the structural safety assessment of a centrifugal compressor impeller, Lerche *et al.* [1] analysed the maximum stress displacement and vibration characteristics when an impeller is subject to the influence of centrifugal force. Park *et al.* [2] examined the effects of changes in the tip gap and impeller blade shape on aerodynamic performance and structural safety of an impeller through FSI analysis. However, few studies have been conducted on a centrifugal compressor impeller considering both aerodynamic performance and structural safety for impeller shape optimization through FSI analysis.

Recently, a great significant of research on optimization methods has been undertaken. Numerical optimization techniques such as multi-objective genetic algorithm methods [3 - 5], gradient-based methods [6], and the response surface method (RSM) in combination with design of experiment (DOE) methods [7, 8] are commonly used for the aerodynamic design of various centrifugal compressors. These methods are useful for analysing the complex correlations between the geometrical parameters and the performance of the fluid machinery.

In this study, the 2nd compressor of multi-stage compressor systems was considered. First, the computational fluid dynamics (CFD) results of a reference model were compared with experimental results. Secondly, one-way FSI analysis was performed using the pressure results of the CFD. Thirdly, optimization with a parametric analysis of the impeller for a 15,000 HP centrifugal compressor was conducted using DOE and RSM. The calculated results were evaluated in terms of isentropic efficiency, total pressure ratio, maximum stress, and total deformation. Finally, the optimal shape of the impeller that gives greater aerodynamic performance and structural safety was suggested.

Received October 29 2015; accepted for publication November 8 2015: Review conducted by Tadashi Tanuma, Ph.D. (Paper number O15057S)
Corresponding author: Youn-Jea Kim, Professor, yjkim@skku.edu

This paper was presented at 13th Asian International Conference on Fluid Machinery (AICFM), September 7-10, 2015, Tokyo, Japan

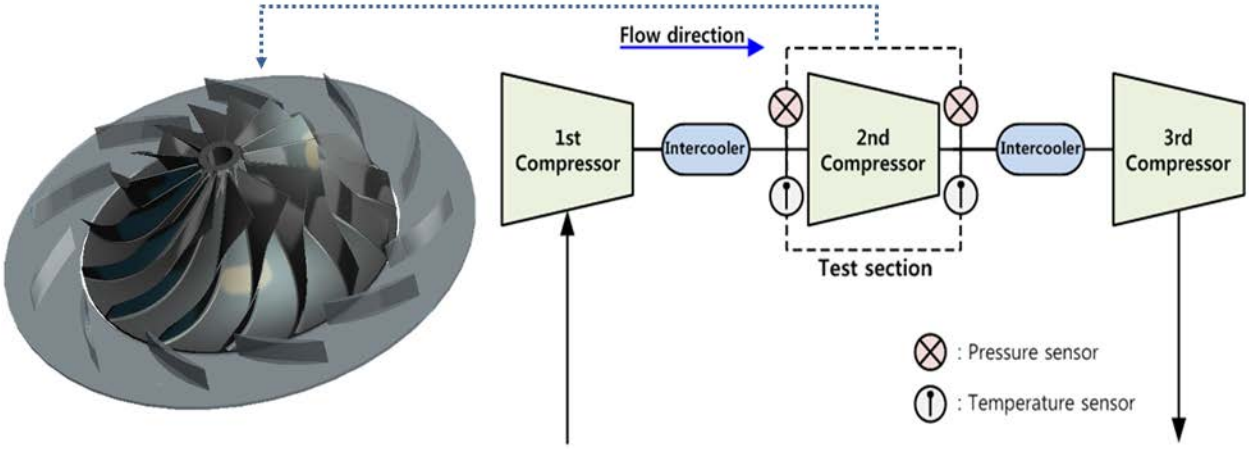

Fig. 1 Schematic of the multi-stage compressor

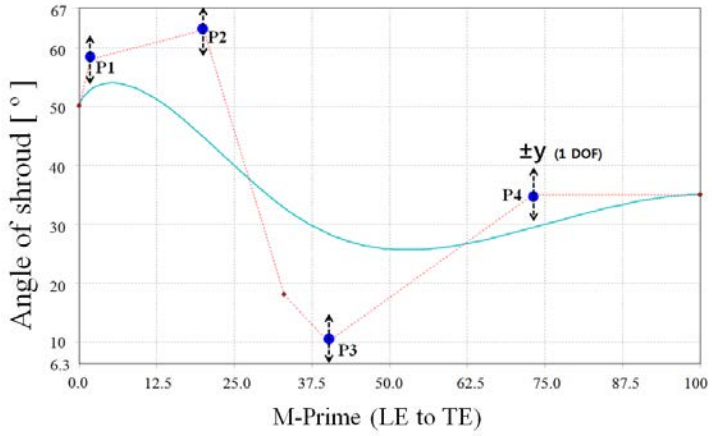

Fig. 2 Control points of the shroud blade angle

2. Fluid-Structure Interaction

2.1 Reference Model

The reference model is shown in Fig. 1. This assembly is part of a multi-stage compressor. The diameter of the centrifugal compressor is 840 mm, and the impeller and diffuser consist of 14 and 11 blades, respectively. The working fluid is an ideal air and the design mass flow rate is 29.7 kg/s at a rotating velocity of 11,417 rpm. At the impeller inlet of the 2nd centrifugal compressor, the stagnation pressure is 237 kPa and the stagnation temperature is 318K. Three-dimensional (3D) geometry was designed by using the ANSYS Blade Editor.

In this research, total of 6 design variables were selected including 4 points (moving towards ±y) on the Bézier-curve, determining impeller shroud curve (see Fig. 2). Table 1 shows the parameterization of the design parameters.

2.2 CFD analysis

Grid systems were generated using ANSYS TurboGrid; these have O-type grids near the blade surfaces and H-type grids in the other regions. In addition, the inflation grid condition was adopted with 10 inflation layers for accurate simulation in the vicinity of the tip clearance. Figure 3 shows the grid systems, which have 1,050,000 and 800,000 elements placed in each passage of the impeller and diffuser, respectively.

The numerical calculations were performed by solving the 3D Navier-Stokes and energy equations using the commercial code, ANSYS CFX 14.5. The calculation domain was chosen to be from the impeller inlet to the diffuser outlet. A steady-state analysis was performed using the κ-ω based shear stress transport (SST) model which has been shown to give relatively accurate predictions in fluid machine analysis [9]. For the boundary conditions, the total pressure and temperature conditions at the impeller inlet were set and a mass flow rate condition was applied at the diffuser outlet. On the other walls, no-slip condition was used. For the case of the interface between the impeller and diffuser, a periodic frozen rotor condition was utilized. The detailed conditions for the CFD analysis are described in Table 2.

In order to calculate the performance of the centrifugal compressor, the isentropic efficiency and the pressure ratio were investigated.

Table 1 Description of design variables

Design variable	Description	Unit	Level 1	Level 2 (Ref.)	Level 3
X_1	Point 1	[˚]	53	58	63
X_2	Point 2	[˚]	58	63	68
X_3	Point 3	[˚]	5	10	15
X_4	Point 4	[˚]	30	35	40

Table 2 Boundary conditions applied in this study

Rotational velocity		11,417 RPM
Fluid		Air ideal gas
Turbulence model		Shear stress transport
Inlet	Pressure	237.3 kPa
Outlet	Temperature	318K
	Mass flow rate	29.7 kg/s
Interface		Frozen rotor
Convergence criteria		1e-4

Table 3 Comparison of the pressure ratio and total temperature between experiments and CFD

	Exp.	CFD
Pressure ratio	1.81	1.85
Exit total temperature	392	390

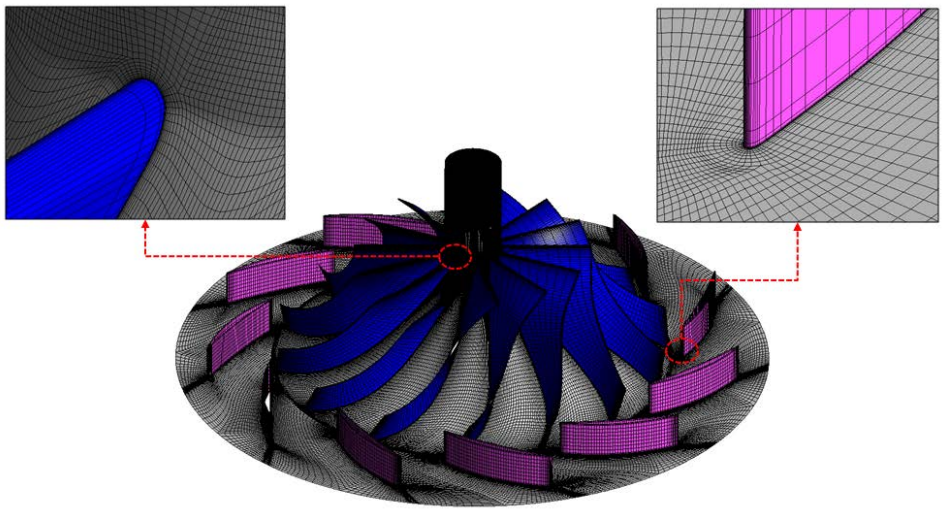

Fig. 3 Grid systems of flow zone

$$\text{Isentropic efficiency, } h = \frac{h_{2s} - h_1}{h_2 - h_1} \tag{1}$$

$$\text{Pressure ratio, } p_R = \frac{\text{outlet pressure}}{\text{inlet pressure}} \tag{2}$$

The isentropic efficiency (η) and the pressure ratio (p_R) were calculated as 86.2% and 1.85, respectively. To validate the CFD results, the pressure ratio and the total temperature at the compressor exit were compared with the existing experiments data and showed good agreement, as outlined in Table 3.

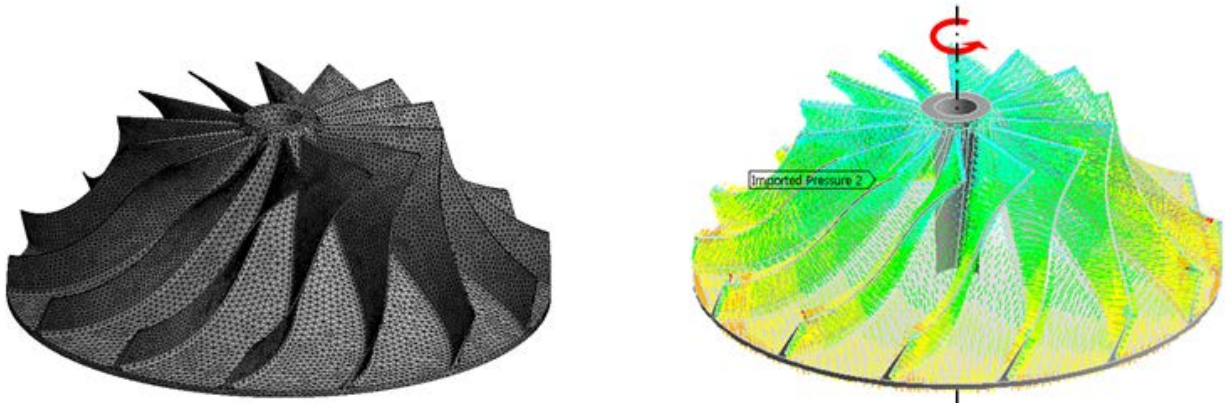

(a) Grid systems of structure zone (b) Pressure distribution on the impeller

Fig. 4 Pre-processing of the FSI analysis

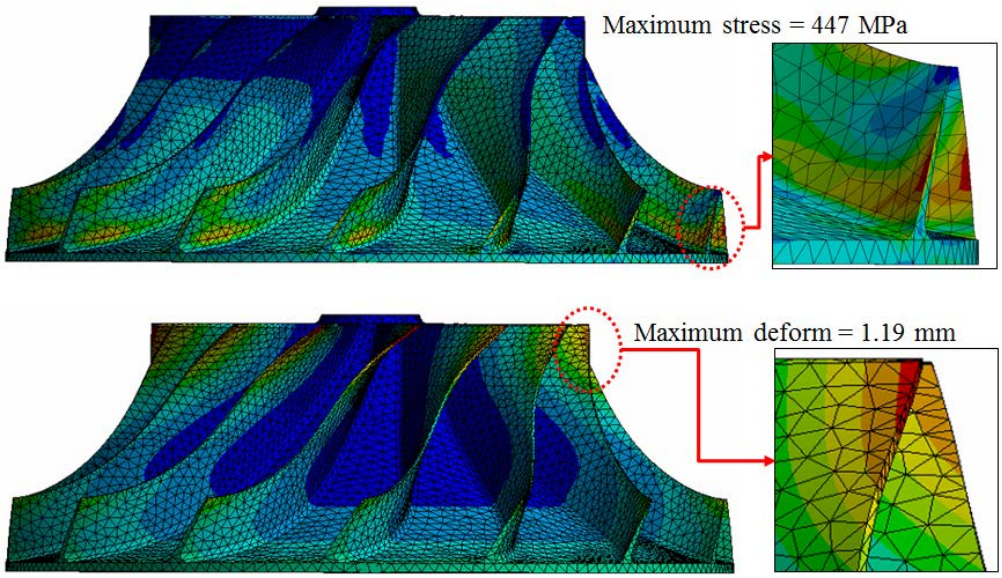

Fig. 5 Results of FSI analysis

Table 4 Parameters of DOE

Design point	X_1	X_2	X_3	X_4	η	σ	p_R
1	57.87	60.27	10.22	38.88	87.48	423	1.8605
2	58.67	62.93	12.44	32.48	86.04	459	2.0215
3	54.13	62.67	12.22	35.52	86.44	424	1.8509
⋮	⋮	⋮	⋮	⋮	⋮	⋮	⋮
23	61.87	58.13	5.88	33.12	86.18	514	1.8964
24	60.27	58.73	7.78	32.96	86.10	444	1.8867
25	62.40	65.07	8.44	37.12	87.01	408	1.9005

2.3 Structural Analysis

Structural analysis was performed using ANSYS Mechanical. The impeller is composed of 17-4ph stainless steel with properties including Young's modulus of 193 GPa, Poisson's ratio of 0.3, and density of 7,750 kg/m^3. For the structure grid, tetrahedron elements were used (see Fig. 4(a)). The impeller axis was fixed as a boundary condition. For the load, the high-velocity rotation centrifugal force and pressure from the CFD analysis were applied to the impeller hub side and blade to perform one-way FSI analysis (see Fig. 4(b)).

Figure 5 shows the result of FSI analysis based on the centrifugal force and fluid pressure. The maximum stress occurring on the impeller was approximately 447 MPa and the maximum displacement was approximately 1.19 mm. The maximum stress occurred in the middle of the blade trailing edge. That location is the same as the commonly reported damaged position of the impeller. The maximum displacement occurred at the end of impeller blade leading edge.

3. Shape Optimization

3.1 Design of Experiment

DOE is a technique that assists in the numerical analysis of performance parameters or in determining an efficient experimental process. By using the Box-Behnken design (BBD) method, the data required for tests can be determined. Therefore, it is possible to maximize the amount of information generated with a minimum number of CFD results. The BBD method consists of the following formula:

$$y = 2k(k - 1) + 1 \tag{3}$$

where y is the number of design points and k is the number of parameters. For the case of 4 parameters, 25 calculation results are required to determine the correlation between the design parameter and the response parameter. The DOE process was conducted by ANSYS Design Xplorer. Table 4 shows the results of the DOE calculations.

3.2 Response Surface Method

The non-parametric regression method (NPR), unlike other RSM methods, does not pass through design points, but estimates the values of the point one needing to be determined. This type of non-parametric regression analysis can remove or decrease error in a given data set. This makes it possible to obtain a regression model closer to the original data [10].

In this study, the root mean square error (RMSE) [11] was used for the response surface appropriateness test, as given in Eq. (4):

$$\mathrm{RMSE}=\sqrt{\frac{1}{N}\sum_{i=1}^{N}(y_i-\hat{y}_i)^2} \tag{4}$$

Here, y_i is the function value of an experimental point's response variable, $\hat{y}_i$ is the function value of the approximate model (response surface) and N represents the number of experimental points for the approximate model evaluation.

3.3 Optimal Design Procedure

In this optimization, the objective function was determined first. The multi-objective genetic algorithm (MOGA) consists of two objective functions, since maximizing the isentropic efficiency and maximum stress for a given design specification was the main objective of this study. Secondly, constraints such as the pressure ratio were determined. The optimization procedures are as follows:

$$\begin{aligned} &\text{Find} && x_i \ (i=1,\ 2,\ 3,\ 4) \\ &\text{To maximize} && \text{Isentropic efficiency, } \eta \\ &\text{To minimize} && \text{Maximum stress, } \sigma \\ &\text{Subject to} && \text{Pressure ratio, } p_R \geq 1.85 \end{aligned} \tag{5}$$

$$\begin{aligned} 53° \leq x_1 \leq 63° \\ 58° \leq x_2 \leq 68° \\ 5° \leq x_3 \leq 15° \\ 30° \leq x_4 \leq 40° \end{aligned}$$

4. Results and Discussion

4.1 Analysis of Sensitivity

Figure 6 presents the sensitivity of the response parameter according to various design parameters using NPR methods. The horizontal axis denotes the input variables with a non-dimensionalized range from 0 to 1. Here the value of the design parameter of the initial model was set to 0.5. For the isentropic efficiency, x_2 and x_3 showed a negative relation to give maximum values at 0.1, ans x_1 to x_4 shows a positive relation. Secondly, at maximum stress, all variables showed a positive relation to give maximum values at 0.9. It can also be noted that the results of the pressure ratio showed a positive relation for x_1, x_2 and x_4. However, the effect of x_3 was relatively small.

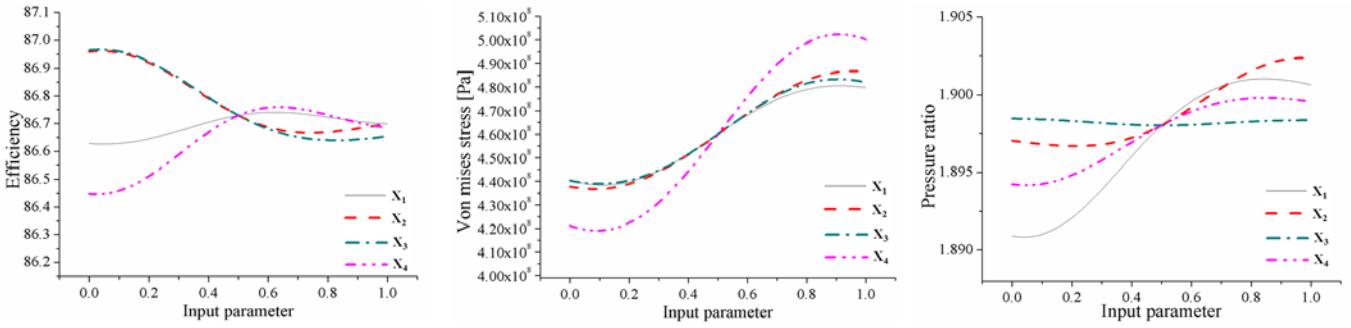

Fig. 6 Results of sensitivity with various design parameters

Table 5 Comparison results between RSM and CFD

Method	x_1	x_2	x_4	x_5	Stress (MPa)	Efficiency	Pressure ratio
RSM (NPR)	60.8	56.8	6.13	31.7	421.9	87.21	1.857
CFD					419.5	87.25	1.856

Table 6 Comparison results between Ref. model and optimal model

	x_1	x_2	x_4	x_5	Stress (MPa)	Efficiency	Pressure ratio
Initial	58	63	10	35	447.4	86.23	1.855
Optimal	60.8	56.8	6.13	31.7	419.5	87.25	1.856

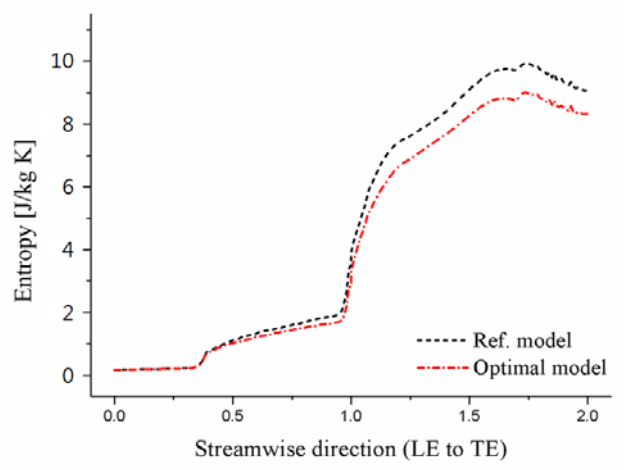

Fig. 7 Comparison results of entropy distribution between the reference model and the optimal model

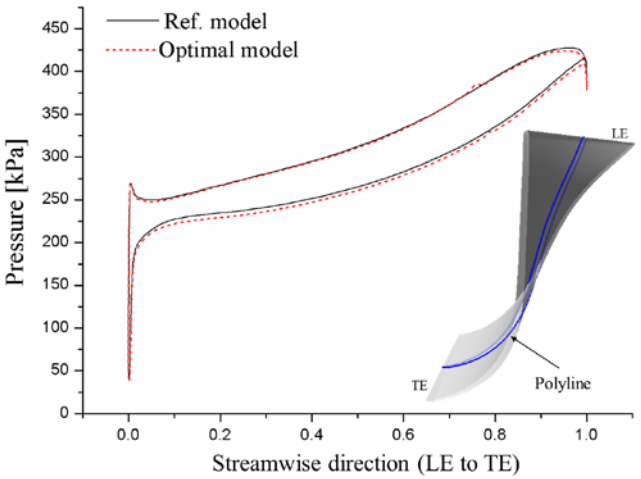

Fig. 8 Comparison results of blade loading distribution between the reference model and optimal model

4.2 Results of Optimal Design

Optimization in this study was carried out using the MOGA method. With the help of the response surface method generated by the NPR method, the optimization results were obtained as shown in Table 5. The relative error for each of the output parameters was 0.04% for the stress, 0.57% for the efficiency and 0.05% for the total pressure ratio. In particular, all approximation models were predicted accurately.

Table 6 shows comparison results between the reference model and the optimal model. The isentropic efficiency, the main

performance of the compressor, was increased by about 1%, while the pressure ratio was maintained at current levels. In addition, at maximum stress, the structural safety parameter was decreased about 6.2%.

Entropy distributions along the streamwise direction of the reference model and the optimal model are shown in Fig. 7. Here, the x-axis denotes the ratio of the impeller inlet to the diffuser outlet. Results show that the optimal model has a lower value of entropy at the diffuser outlet than the reference model. Since the outlet entropy represents the total amount of loss accumulated in the passage, the isentropic efficiency value of the optimal model should be higher than that of the reference model.

Figure 8 shows the comparison results of the blade loading distribution on the impeller polyline between the reference model and optimal model. It shows that the loading pressure of the optimal model was smaller than that of the initial model. Especially, the peak pressure was reduced at the trailing edge(TE). This is the reason why the optimal model gave a smaller maximum stress value.

5. Conclusions

In this study, the optimal shape design for a centrifugal compressor impeller was determined using RSM and DOE in combination with the BBD method. In particular, the influence of the design parameters on the isentropic efficiency, pressure ratio, and stress was analyzed. In addition, the correlations between the design variables and output parameter were investigated.

Through the optimization, when the current level pressure ratio is maintained, the optimal designed model showed that the efficiency, which is the main performance parameter of the centrifugal compressor, was increased by about 1%. In addition, at maximum stress, the structural safety parameter was decreased by 6.2%.

Nomenclature

p	Static pressure	LE	Leading edge
p_o	Total pressure	TE	Trailing edge
η	Isentropic efficiency	σ	Maximum stress
p_R	Pressure ratio	BBD	Box-Behnken design

References

[1] A. H. Lerche, J. J. Moore, N. M. White and J. Hardin, “Dynamic stress prediction in centrifugal compressor blades using fluid structure interaction,” Proceeding of ASME Turbo Expo, Vol. 6, pp. 193-200, 2012.

[2] Park, T. G., Jung, H. T., Kim, H. B. and Park, J. Y., 2011, "Numerical study on the aerodynamic performance of the turbo blower using fluid-structure interaction method," Journal of the Korea Society for Power System Engineering, Vol. 15, No. 6, pp. 35~40 (in korean).

[3] J. H. Kim, J. H. Choi, A. Husain and K. Y. Kim, “Multi-objective optimization of a centrifugal compressor impeller through evolutionary algorithms,” J. Power and Energy, Vol. 224, pp. 711–721, 2010.

[4] J. H. Kim, J. H. Choi and K. Y. Kim, “Design optimization of a centrifugal compressor impeller using radial basis neural network method,” Proceeding of ASME Turbo Expo, Vol. 7, pp. 443-451, 2009.

[5] Benni, E. and Pediroda, V., “Aerodynamic optimization of an industrial centrifugal compressor impeller using genetic algorithm,” Proceeding of Eruogen, pp. 467-472, 2001.

[6] X. F. Wang, G. Xi and Z. H. Wang, “Aerodynamic optimization design of centrifugal compressor’s impeller with Kriging model,” J. Power and Energy, Vol. 220, pp. 589–597, 2006.

[7] S. M. Kim, J. Y. Park, K. Y. Ahn, and J. H. Baek, “Numerical investigation and validation of the optimization of a centrifugal compressor using a response surface method,” J. Power and Energy, Vol. 224, pp. 251–259, 2009.

[8] D. Bonaiuti, A. Arnon, M. Ermini, and L. Baldassarre, “Analysis and optimization of transonic centrifugal compressor impellers using the design of experiments technique,” ASME J. Turbomach., Vol. 128, No. 4, pp. 786-797, 2006.

[9] J. E. Bardina, P. G. Huang, and T. Coakley, “Turbulence modeling validation,” 28th AIAA Fluid Dynamics Conference, AIAA-1997-2121, 1997.

[10]P. J. Greem and B. E. Silverman, “Nonparametric regression and generalized linear models,” New York: Chapman & Hall, 1994.

[11] B. H. Ju, T. M. Cho, D. H. Jung and B. C. Lee, “An error assessment of the Kriging based approximation model using a mean square error,” Trans. Korean Soc. Mech. Eng. A, Vol. 30, No. 8, pp. 923-930, 2006 (in korean).